


Research

Novel multiphase loop reactor with improved aeration prevents excessive foaming in Rhamnolipid production by *Pseudomonas putida*

Maximilian von Campenhausen¹  · Philipp Demling²  · Patrick Bongartz³  · Alexander Scheele³ · Till Tiso²  · Matthias Wessling^{3,4}  · Lars M. Blank²  · Andreas Jupke¹ 

Received: 26 October 2022 / Accepted: 5 January 2023

Published online: 18 January 2023

© The Author(s) 2023 

Abstract

Rhamnolipids are biosurfactants that tend to cause strong foaming, making microbial production in an aerated stirred tank fermenter challenging. The continuous removal of rhamnolipids from the cultivation broth via *in situ* liquid-liquid extraction can remedy this foam challenge, and thereby supports long-term cultivation and production. However, for efficient processing and stable phase separation, a specialized apparatus is required. In this study, the novel multiphase loop reactor, which is a modified airlift reactor with an internal loop enabling continuous *in situ* liquid-liquid extraction, was designed and adapted to produce rhamnolipids with a recombinant bacterium, *Pseudomonas putida* KT2440. The initially designed multiphase loop reactor showed a low oxygen transfer rate, unable to meet the oxygen demand of the whole-cell biocatalyst, resulting in inefficient growth and production. A re-design of the sparger via 3D printing enabled a high oxygen supply allowing rhamnolipid production at key performance indicators that matched stirred-tank reactor cultivations. Advantageously, the multiphase loop reactor allowed stable and constant phase separation and solvent removal enabling continuous cultivation in the future. Concluding, the successful use of the multiphase loop reactor for rhamnolipid synthesis is presented, highlighting its potential to become a new platform technology for intensified bioprocessing.

Keywords In situ liquid-liquid extraction · Multiphase loop reactor · Platform technology · Rhamnolipids · *Pseudomonas putida* · Aeration · 3D-printing

1 Introduction

Foaming is one of the major challenges in bioprocessing as it influences many cultivation conditions, e.g., the lack of nutrient supply for whole-cell biocatalysts residing in the foam [1]. Thereby, inhomogeneities in the reactor and within the microbial population are induced. In severe cases, excessive foaming causing the reactor to overflow

Maximilian von Campenhausen and Philipp Demling contributed equally to this work.

Supplementary Information The online version contains supplementary material available at <https://doi.org/10.1007/s43938-023-00018-5>.

✉ Andreas Jupke, Andreas.Jupke@avt.rwth-aachen.de | ¹Fluid Process Engineering (AVT.FVT), RWTH Aachen University, 52074 Aachen, Germany. ²Institute of Applied Microbiology (iAMB), Aachen Biology and Biotechnology (ABBt), RWTH Aachen University, 52074 Aachen, Germany. ³Chemical Process Engineering (AVT.CVT), RWTH Aachen University, 52074 Aachen, Germany. ⁴DWI Leibniz - Institute for Interactive Materials, 52074 Aachen, Germany.



results in a loss of whole-cell biocatalysts accumulated in the foam [2], poor process control [1], and most often in a termination of the cultivation [3].

There are different measures to handle excessive foam either by foam destruction (chemical [4] or mechanical [5]) or foam prevention by bubble-free aeration [6] or anti-foam agents [7]. Further, the foam has been used as an advantage to isolate the product by a controlled outflow [8, 9]. Another approach to isolate the product and simultaneously prevent excessive foam formation is *in situ* liquid-liquid extraction of the component [10], which causes foaming. The product isolation during the process enables continuous production and additionally intensifies the cultivation by integrating the first downstream unit operation into the bioreactor.

Reactors with integrated *in situ* liquid-liquid extraction have been assessed previously in different designs [10, 11]. Simple reactor setups used are conventional stirred-tank reactors (STRs) operated in batch mode with both aqueous and solvent phases homogeneously mixed. The phases are separated after cultivation [12, 13]. A two-liquid phase batch cultivation of *P. putida* KT2440 SK4 with ethyl decanoate as a solvent in STRs has been previously conducted for the production of the foam-inducing class of biosurfactants rhamnolipids (RL) and identified a reduction of the pH value to enhance *in situ* liquid-liquid extraction and prevent excessive foaming, although partially compromising growth and production [14]. Ethyl decanoate as an extraction solvent was specifically selected for the bioprocess based on its partition coefficient, biocompatibility, safety, recyclability, and settling behavior. However, the introduction of cultivation concepts with an integrated continuous circulation of ethyl decanoate removing RL has been predicted to further improve the overall efficiency.

Some reactors enable the continuous removal of the solvent phase during the cultivation by integrating a settler compartment in the reactor [15, 16]. The continuous removal allows the replacement of saturated solvent. This keeps the driving force for liquid-liquid extraction high and therefore, the concentration of foaming or, in general, inhibiting components low [17]. Furthermore, the replacement is a prerequisite for a full continuous mode for integrated apparatuses including continuous aqueous feed and purge.

However, *in situ* liquid-liquid extractions in stirred bioreactors often result in the formation of stable emulsions due to peaks in shear stress, which cause highly dispersed solvent drops [18]. Analogously to foam withdrawal [19], continuous removal of the emulsion would lead to the loss of whole-cell biocatalyst, thereby reducing the efficiency of the fermentation process. Therefore, the presence of a coherent solvent phase is necessary to enable continuous solvent removal while retaining the whole-cell biocatalysts in the reactor. This requires a reactor setup exhibiting reduced and homogeneously distributed shear stress. Solvent drops would be larger and more homogenous in size which enables faster coalescence to form a coherent solvent phase [20]. The solvent could be withdrawn from the reactor leaving the whole-cell biocatalysts in the aqueous phase.

The novel multiphase loop reactor (MPLR) is based on a non-stirred airlift reactor (ALR) advanced by an integrated *in situ* liquid-liquid extraction to allow simultaneous microbial production and continuous product removal [21]. ALRs are commonly applied in biotechnology and wastewater treatment and excel by low and homogenous shear stress compared to STRs [22]. By transferring this feature to the novel MPLR, stable emulsions are prevented allowing easier phase separation and solvent recirculation compared to STRs.

The process intensification by the combination of cultivation and liquid-liquid extraction in the MPLR exceeds sole savings in space at the production site [23]. The intensification also reduces repeated anaerobic residence times for whole-cell biocatalysts compared to a segmented process with an external loop. In a segmented process, the anaerobic residence time enlarges quickly with piping coupling operational units for cultivation and liquid-liquid extraction. Additionally, cell retention, commonly applied for *in situ* liquid-liquid extraction with an external loop to prevent the organisms from excessive anaerobic residence times, is not required [10]. Regarding anaerobe residence times in the MPLR, it was previously shown that a short-term oxygen limitation, the obligate aerobe organism *P. putida* might be exposed to in the MPLR, only influences the productivity due to moderately slower growth and production while the final biomass and product titers remain unaltered [24].

The MPLR with its unique features, most prominently low solvent drop breakage for internal phase separation and continuous solvent recirculation, is a promising reactor to enable continuous multiphase bioprocesses for *in situ* liquid-liquid extractions. Thereby, the described advantages of continuously removing inhibiting products can be exploited. For the first time, the MPLR is applied to support a microbial production process at a 5 L-scale. The feasibility of the MPLR concept enabling *in situ* liquid-liquid extraction with continuous solvent removal to cultivate

the recombinant bacterium *Pseudomonas putida* KT2440 SK4, previously engineered to produce rhamnolipids (RL), a class of biosurfactants [25, 26], is assessed. To avoid excessive foaming due to the produced RL, the advantageous characteristics of the MPLR are utilized and aeration is improved.

2 Materials and methods

2.1 Reactor design

The MPLR is based on the principle of an internal loop reactor. A concentric cylinder separates the downcomer and the riser zone. The aeration in the riser induces the loop flow of a continuous phase, the medium, pictured in Fig. 1a. In the downcomer, a dispersed organic liquid phase, the solvent, rises in counter-flow to the medium to the surface due to a lower density. The solvent extracts compounds from the medium during sedimentation. Inside a 100 mm tall settler compartment (marked blue in Fig. 1c) at the top of the downcomer, an unstructured stainless-steel mesh with pore sizes around 2 mm attenuates turbulences and enhances the coalescence of the solvent. A continuous outlet (\varnothing 4 mm) for withdrawing the solvent is fixed in the settler compartment slightly above the liquid surface to maintain the filling volume at a constant level. The wall of the settler compartment extending 63° of the circumference of the inner cylinder prevents the cultivation broth, accelerated by the loop flow, to enter the settling zone.

The 5 L reactor glass vessel was made by Eppendorf SE (Hamburg, Germany). The in-house manufactured head-plate and stand enable the setup of the MPLR-specific internals. The internals are a cylinder, a disperser for the solvent feed at the base of the reactor, a settler compartment, and a pipe for solvent withdrawal. All these internals are made of stainless steel (material no. 1.4404). The cross-sectional areas of the riser and a downcomer are at a ratio of 1:2.1. The dimensions of the reactor and selected internals can be drawn from Fig. 1b.

Regarding the sparger, three different designs were used (Fig. 2a–c). The ring sparger (a) and the frit sparger (b) are made of stainless steel (material no. 1.4404). The ring sparger consists of three interconnected ring pipes with upward-facing holes equally distributed across the lower cross-section of the riser. The frit sparger is a sintered stainless-steel frit covering only a fraction of the cross-section of the riser. The PAM sparger (c) evenly distributes bubbles across the lower cross-section of the riser through a 3D printed porous poly(dodecane-12-lactam) (PA 12) spiral with a porosity of 15% and pore diameters ranging from 0.7 to 8.0 μm [27].

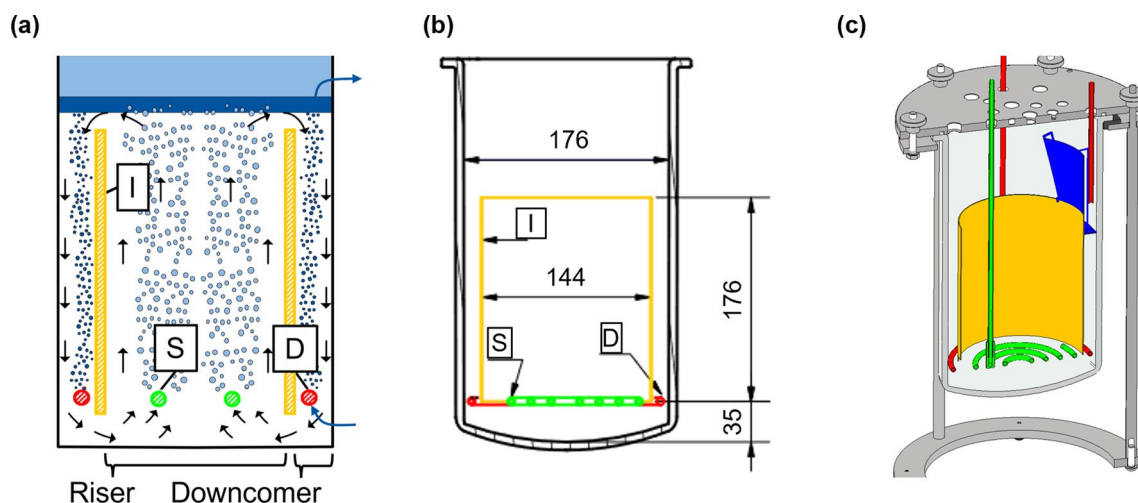


Fig. 1 Reactor design with inner cylinder (I, yellow), sparger (S, green), and disperser (D, red): **a** flow principle of the MPLR (white background and black arrows: aqueous phase, dark blue background and blue arrows: solvent phase, light blue background: air), **b** MPLR dimensions in mm and **c** half section view of MPLR with settler compartment in blue

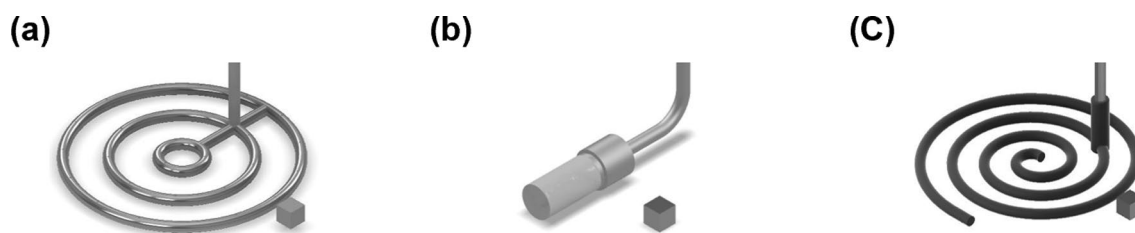


Fig. 2 Sparger designs with 1 cm reference cube: **a** stainless-steel ring sparger (27 holes, \varnothing 1 mm); **b** stainless-steel sintered frit (\varnothing 17 mm, 32 mm length, pores \varnothing 10 μ m); **c** sintered PAM spiral sparger [27]

2.2 Reactor setup

The setup of the MPLR for cultivations is depicted in Fig. 3. The probes in the MPLR are connected to two linked BioFlo110 control units.¹ Each unit controls one compartment enabling the individual control of the downcomer and riser. Both compartments contain a temperature, an invasive DO,² and a pH³ probe each. Temperature and pH probes of either compartment can be used for control. The set temperature is maintained by a cooling coil and a heating blanket. Both, the flow through the cooling coil and the power of the heating blanket, can be controlled via either control unit. The pH is controlled with acid and base addition through two internal peristaltic pumps of the control unit receiving signals from the corresponding pH probe. A peristaltic pump⁴ (P2) transports the solvent from the 1.5 L solvent reservoir through the disperser into the MPLR. In the settler compartment, a height-adjustable tube constantly withdraws either gas or solvent through another external peristaltic pump (P1), retaining a constant liquid filling volume. For solvent-contacting equipment, solely polytetrafluoroethylene (PTFE), stainless steel, and boron-silicate glass were used to ensure resistance against the solvent. Any mixtures of gas can be chosen (in this setup nitrogen and air) to enter the MPLR through the sparger. The gas flow is controlled by two thermal mass flow controllers⁵ connected via a 4–20 mA controller linked to the BioFlo110 control units. An online analytical device⁶ measures oxygen and carbon dioxide concentrations in the exhaust gas. All equipment potentially contaminated by organisms is autoclavable.

2.3 Bacterial strain and cultivation method

P. putida KT2440 SK4 with $attTn7::P_{ffg}-rhlAB$ was constructed and characterized in previous studies [25, 26]. It is a RL-producing whole-cell biocatalyst, which tolerates temporary oxygen depletion [24]. Its chassis strain, *P. putida* KT2440 [28–30], is classified as a host-vector system with safety level 1 (HV1).

Cells were retrieved from cryopreserved cultures (20% (v/v) glycerol in lysogeny broth) on agar plates. Lysogeny broth (5 g L⁻¹ yeast extract, 10 g L⁻¹ tryptone, 5 g L⁻¹ NaCl) was inoculated with a single colony for the first seed culture, which was incubated at a temperature of 30 °C and a shaking frequency of 300 rpm. The secondary seed culture was incubated at the same conditions and cells were grown until mid-exponential phase before transferring to the production culture in the bioreactor. For secondary seed cultures and production cultures, a mineral salts medium (MSM) adapted from Hartmans et al. [31] (Table 1) was used. *P. putida* KT2440 produces gluconate, which causes a decrease in pH value. To stabilize the pH value, phosphate buffer (K₂HPO₄/NaH₂PO₄) was added as part of the medium (Table 1). For the production cultivation in the bioreactor, the pH value could be actively controlled by the addition of acid or base. Therefore, the concentration of the buffer was lowered to a third of its initial concentration.

Protocols for STR cultivations of *P. putida* established by Demling et al. [14] were adapted for the MPLR. Here, 4 L of MSM were inoculated to an optical density (OD₆₀₀) of 0.2. RLs produced by *P. putida* KT2440 SK4 were isolated by liquid-liquid extraction with 1100 mL of ethyl decanoate as the solvent, which was dispersed at a flow rate of 10 mL min⁻¹ and finally withdrawn from the coherent solvent phase in the settler compartment. The pump for withdrawal was set

¹ Eppendorf SE (Hamburg, Germany).

² VisiFerm by Hamilton Company (Bonaduz, Switzerland).

³ phferm by Hamilton Company (Bonaduz, Switzerland).

⁴ Masterflex L/S Variable-Speed Drive by Cole-Parmer GmbH (Wertheim, Germany).

⁵ EL Flow Select F-201CV-20 K-AGD-00-V by Bronkhorst Deutschland Nord GmbH (Kamen, Germany).

⁶ BlueVary, BlueSens GmbH (Herten, Germany).

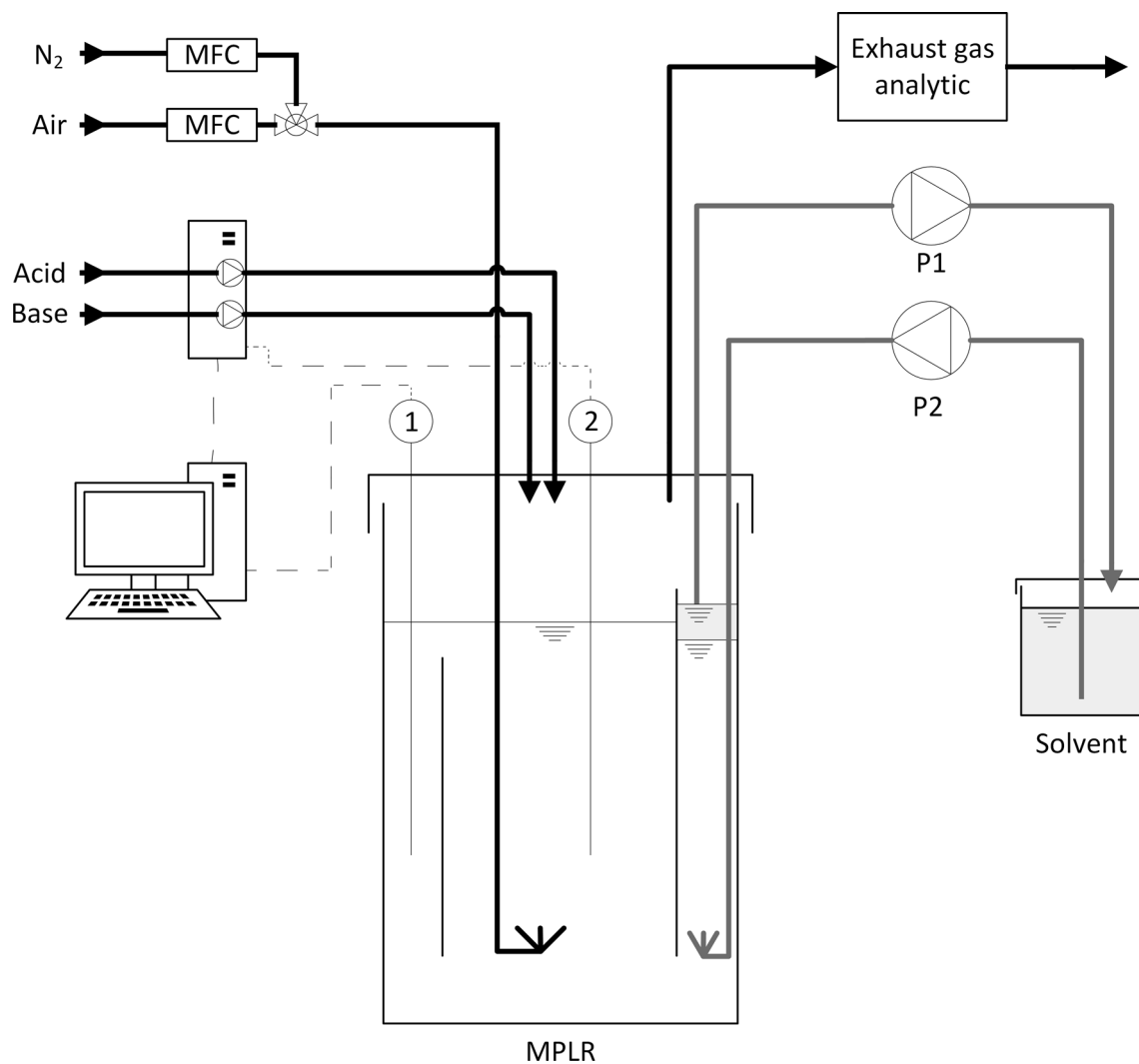


Fig. 3 Schematic illustration of the MPLR setup. For simplicity, DO, pH, and temperature probes are collectively pictured as one probe for the downcomer (1) and one probe for the riser (2). Solvent and solvent-related equipment are pictured in grey

Table 1 Components of MSM modified from Hartmans et al. [31]

Amount	Component	Amount	Component
10	g L ⁻¹	1	mg L ⁻¹
11.64	g L ⁻¹	5	mg L ⁻¹
4.89	g L ⁻¹	0.2	mg L ⁻¹
2	g L ⁻¹	0.2	mg L ⁻¹
0.1	g L ⁻¹	0.4	mg L ⁻¹
10	mg L ⁻¹	1	mg L ⁻¹
2	mg L ⁻¹		

to 20 mL min⁻¹. During the cultivation, half of the solvent remained in the solvent storage tank. The solvent does not need to be autoclaved before use in the cultivation. For pH control, the probe installed in the riser was used. Adapting the findings by Demling et al. [14] describing that a lower pH value enhances the RL extraction, the set pH value was decreased by hand when accumulated foam was on the verge of entering the settler compartment. Aeration with air in the riser was adjusted within the range of 0 – 20 L_N min⁻¹ depending on the dissolved oxygen tension (*DOT*). Thereby,

sufficient oxygen supply for microbial growth was ensured during the cultivation. The temperature was kept stable at 30 °C and was controlled based on the temperature measured in the downcomer.

2.4 Quantification of extracellular metabolites

For RL quantification, a High-Performance Liquid Chromatography (HPLC)⁷ system with a reversed-phase column⁸ and a Corona Veo Charged Aerosol Detector⁹ was used. A nitrogen generator¹⁰ supplied a constant nitrogen flow for the detector. A previously described method was applied [32]. Two buffers, (A) acetonitrile and (B) 0.2% (v/v) formic acid in double-distilled, purified water were used for gradient elution. The measurement period per sample was 15 min. For 1 min, the starting conditions were kept constant at 70% (v/v) buffer A and 30% (v/v) buffer B. Next, buffer A was gradually elevated to a fraction of 80% (v/v) over a period of 8 min. Subsequently, the fraction of buffer a was increased to 100% (v/v) within 1 min, at which it was kept stable for 1 min. Thereafter, the fractions were reversed to the starting conditions within 1.5 min, without further alterations until the end of the measurement period. The column oven temperature and the flow rate were set to 40 °C and 1 mL min⁻¹, respectively. A sample volume of 5 µL was injected. Four HAA congeners and four mono-RL congeners could be detected and quantified.

If necessary, aqueous samples were set to a pH value of 7 by titrating with 1 M KOH or 1 M HCl. Thereby, quantification bias was prevented. Aqueous samples were treated with acetonitrile in equal volumes to precipitate proteins. The samples were mixed and incubated for more than 4 h at 4 °C. Subsequent centrifugation (21,000 g, 3 min) and filtration¹¹ removed precipitated proteins. For the preparation of solvent samples, a vacuum, 60 °C, and 1,400 rpm¹² were applied to evaporate the organic phase. A 50% (v/v) acetonitrile-double distilled water solution was used to resolve dried residuals.

To quantify glucose and the intermediates gluconate and 2-ketogluconate, the samples were centrifuged (21,000 g, 3 min) and filtered.¹³ A volume of 10 µL of the supernatants was injected into an HPLC system⁷ with a chromatography column for acids, alcohols, and carbohydrates,¹⁴ coupled to a Variable Wavelength Detector¹⁵ set to 210 nm and an additional refractive index (RI) detector.¹⁶ The RI detector was used to quantify glucose, while gluconate and 2-ketogluconate were quantified via the Variable Wavelength Detector. Elution was performed isocratically. The flow rate of the running buffer (5 mM H₂SO₄) was set to 0.6 mL min⁻¹, and the column temperature was kept at 40 °C.

2.5 Volumetric oxygen mass transfer coefficient

The oxygen mass transfer coefficient ($k_L a$) is the apparatus-specific parameter to describe the oxygen transfer rate (OTR) from the gaseous to the liquid phase according to the two-film theory [33]. The coefficient describes the change of the dissolved oxygen concentration in the liquid phase in relation to the difference between the saturated ($C_{O_2}^*$) and actual dissolved oxygen concentration (C_{O_2}) in the liquid phase. Expressed as a balance equation neglecting microbial oxygen consumption results in Eq. (1). Assuming a constant $C_{O_2}^*$ and dividing Eq. (1) by $C_{O_2}^*$, the mass transport can be expressed as Eq. (2) using the normalized dissolved oxygen concentration in the liquid phase, the DOT . The change of the DOT over time equals the oxygen transfer rate (OTR , Eq. (3)). Analogous to the OTR , the carbon transmission rate (CTR) describes the carbon, *i.e.*, carbon dioxide, transport from the liquid to the gaseous phase.

$$\frac{dC_{O_2}}{dt} = k_L a (C_{O_2}^* - C_{O_2}) \quad (1)$$

⁷ DIONEX UltiMate 3000 by Thermo Fisher Scientific (Waltham, USA) composed of pump module LPG-3400SD, autosampler WPS-3000 (RS), and the column oven TCC-3000 (RS).

⁸ NUCLEODUR C18 Gravity 150 × 4.6 mm separation column, particle size: 3 µm by Macherey–Nagel GmbH & Co. KG (Düren, Germany).

⁹ Corona Veo Charged Aerosol Detector by Thermo Fisher Scientific (Waltham, USA).

¹⁰ Parker Balston NitroVap-1LV by Parker Hannifin GmbH (Kaarst, Germany).

¹¹ Phenex RC syringe filters, pore size: 0.2 µm, d = 4 mm by Phenomenex (Torrance, USA).

¹² ScanSpeed 40 attached to ScanVac Coolsafe 110–4, both by Labogene ApS (Lyngø, Denmark) and Chemistry Hybrid Pump RC 6 by vacuubrand GmbH + Co. KG (Wertheim, Germany).

¹³ Phenex RC syringe filters, pore size: 0.2 µm, d = 4 mm by Phenomenex (Torrance, USA).

¹⁴ ISERA Metab AAC 300 × 7.8 mm separation column with a particle size of 10 µm by ISERA GmbH (Düren, Germany).

¹⁵ DIONEX UltiMate 3000 Variable Wavelength Detector by Thermo Fisher Scientific (Waltham, USA).

¹⁶ SHODEX RI-101 RI detector by Showa Denko Europe GmbH (Wiesbaden, Germany).

$$\frac{dDOT}{dt} = k_L a (1 - DOT) \quad (2)$$

$$OTR = \frac{dDOT}{dt} \quad (3)$$

In general, for non-limited cultivations, the development of the *OTR* and *CTR* is exponential over time under the premise that the cells grow exponentially and are homogeneous regarding their respiratory activity. A semi-logarithmic plot reveals changes in the logarithmic slope and therefore changes in the exponent indicating disturbance or improvement of the organism-specific respiratory activity.

To determine the $k_L a$, a method suggested by DECHEMA¹⁷ as standard [34] was used. Accordingly, the *DOT* is measured during the aeration of the previously deoxygenated medium and fitted to Eq. (2). For deoxygenation, pure nitrogen gas was applied to strip the oxygen from the medium until the DO-probe output signal was constant. This value was set to a *DOT* of 0%. Subsequently, the sparged gas was switched back to air. The resulting incline of the *DOT* was used for the fit, whereas the maximum of the output signal from the DO-probe corresponds to a *DOT* of 100%.

Parameters influencing the $k_L a$ are the reactor geometry, operating parameters, and the used material system [35]. To compare different reactor setups a PBS buffer (composition in Supplementary Information, Table S1) has been defined as standard [34]. Thus, it was used in this study. The PBS buffer mimics physical properties like the viscosity and density of a cultivation system.

The $k_L a$ for the ring sparger, the frit sparger, and the PAM sparger were determined for 1 and 2 vvm at the same filling volume (4 L) at which the cultivations were conducted. The determination was repeated five times.

2.6 Characterization of bubble size distributions

Bubble size distributions to further understand the dependence of the $k_L a$ on the type of sparger were determined. Instead of the opaque stainless-steel cylinder, a geometric similar inner cylinder made of glass was inserted in the middle of the reactor. Internals for fixating the glass cylinder had to be adjusted slightly due to the change in the cylinder material. Bubbles were approximated as oblate spheroids. Thereby, the two principal diameters were manually measured by correlating the distance and pixel of a taken picture at a defined space in the middle of the riser. The validation by the measurement with a reference length in the evaluated space precluded a significant impact of the optical length distortion of the picture due to the change of optical density between the glass and PBS buffer and due to the curved glass vessel.

A characteristic value of particle size distributions is the Sauter mean diameter (d_{32}). The d_{32} depicts the diameter of equally sized spheres, which have the same surface area, and volume of the examined particles [36] - here bubbles. Deriving from the definition, the d_{32} is calculated by Eq. (4)

$$d_{32} = \frac{\sum_i d_i^3}{\sum_i d_i^2} \quad (4)$$

whereas each bubble diameter d_i was calculated from the average of the principal diameters of the bubbles.

To characterize the bubble size distribution of the ring sparger, the frit sparger, and the PAM sparger, six different aeration rates ranging from 0.5 to 3 vvm were examined in a 5 cm by 5 cm plane located 2 cm above the sparger in the center of the reactor after stationary fluid dynamics have been established visually. For the aqueous medium the same volume (4 L) of PBS buffer, also used for determining the $k_L a$ (see above), was used.

¹⁷ DECHEMA Gesellschaft für Chemische Technik und Biotechnologie e.V. (Frankfurt a.M., Germany).

3 Results

3.1 Reference cultivation with ring sparger assesses the functionality of the MPLR

This cultivation was the first time the MPLR was applied for microbial production. The protocol was based on previously performed benchmark cultivations in STRs and experiments assessing the coalescence performance [14]. The resulting data for the *DOTs* in the riser and downcomer, *OTR*, *CTR*, respiratory quotient (*RQ*), pH value, and concentrations in the phases are plotted in Fig. 4a-d.

Although the basic MPLR concept regarding fluid dynamics worked visually as intended, the *DOT* values decreased rapidly in both compartments within 78 min after inoculation. The *DOT* value in the riser decreased below 30%, while the *DOT* in the unaerated downcomer reached even lower values of approximately 10%. Both signals indicate that the *OTR* hardly satisfies the oxygen demand of the cells already shortly after inoculation. Although increasing the aeration rate at 78 min from 3.2 to 4.8 L min⁻¹ (0.8 to 1.2 vvm) resulted in enhanced *DOT* values in both the riser and the downcomer, this was only a temporary alleviation, as eventually the *DOT* decreased to 0% after 160 min in the downcomer and after 210 min in the riser. Thus, the cells were exposed to oxygen limitation in both compartments.

Consequently, the production of RL was limited. The concentration of RL did not increase for at least 130 min. After this unproductive phase, the concentration of RL in the circulating organic phase increased to 640 mg L⁻¹. Notably, the produced RL were successfully extracted keeping the concentration in the aqueous phase at constantly low values between 20 and 30 mg L⁻¹.

The reactor could be operated until 230 min without a significant amount of foam in the headspace. Afterward, increasing RL concentrations led to excessive foam formation. For the STR benchmark cultivation, it was shown that lower pH values result in higher partition coefficients for RL when extracted with ethyl decanoate. Higher affinity to

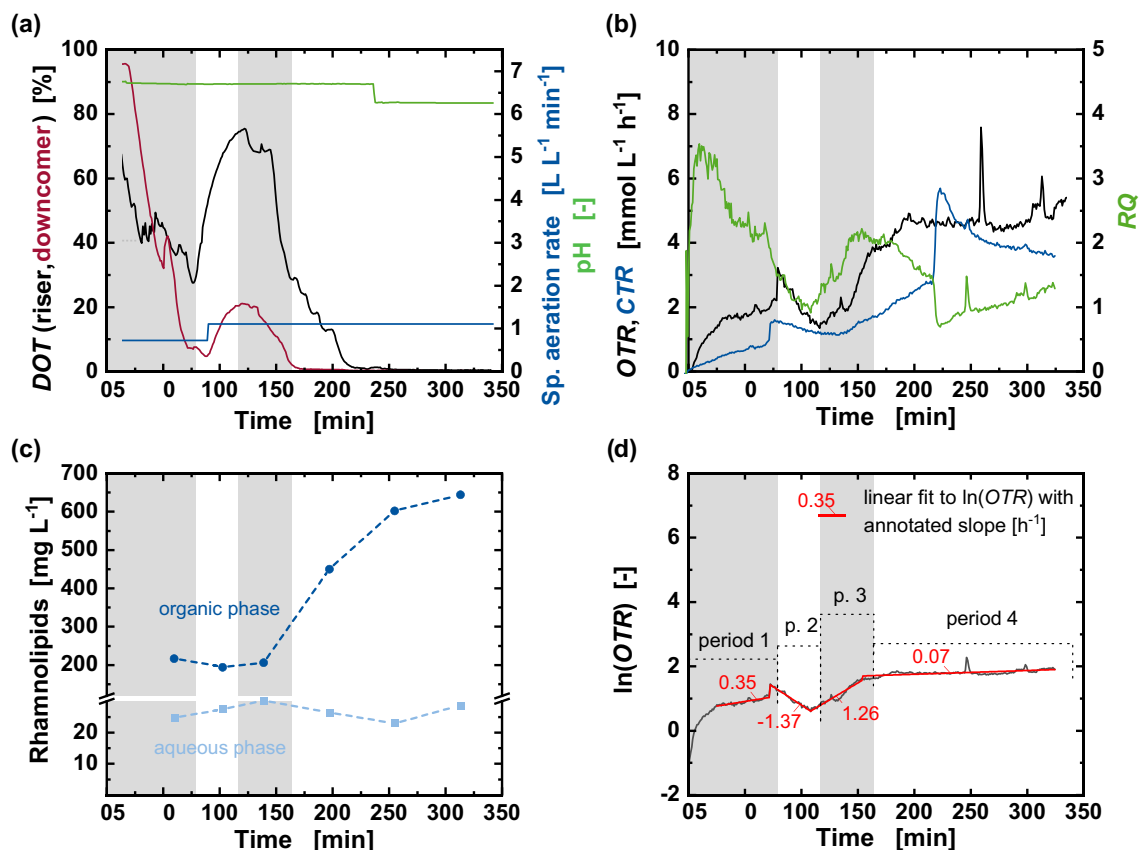


Fig. 4 Kinetic of *P. putida* KT2440 SK4 cultivation in the MPLR. **a** *DOTs*, specific aeration rate, pH, **b** *OTR*, *CTR*, *RQ* **c** concentration of RLs in aqueous (light blue) and organic phases (dark blue), and **d** the logarithmic *OTR* with a linear fit and marked slopes over time. The shaded background mark periods as annotated in **d** depending on the slope of the linear fit to $\ln(OTR)$

the solvent is hypothesized to be attributed to the lower polarity of the protonated form of RL [14]. Adapting this strategy, the pH value was reduced here, too. A decrease from a pH value of 7 to 6.5 resulted in the intended collapse of the foam preventing any further foaming during the remaining cultivation.

The sudden decrease in pH value also shifted the dissociation equilibrium between the carbon dioxide and carbonic acid to the prior. Due to the degassing of unsolvable carbon dioxide, the *CTR* increased rapidly (Fig. 4b). However, this effect was limited to immediately after acid addition. Further, the *CTR* increased at 78 min after inoculation, simultaneously with the increase of the aeration rate. This *CTR* increase is caused by a non-microbiological effect, as the higher aeration rate stripped additional carbon dioxide from the cultivation broth and the solvent. However, this disequilibrium leveled during the following 60 min.

Although the biomass concentration could not be measured due to the present ethyl decanoate, growth can be qualitatively estimated by the *OTR* development during the cultivation. However, different overlaying phenomena influencing the metabolism, solubility, and concentration profiles in the MPLR led to an inconclusive *OTR* signal, and consequentially an ambiguous respiratory quotient (*RQ*).

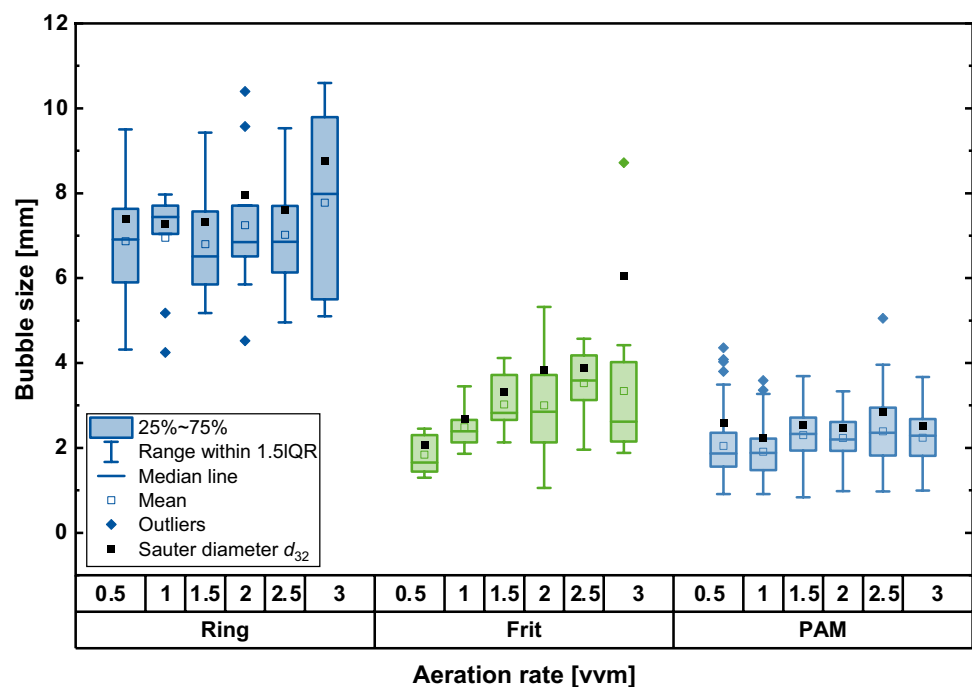
The cultivation was terminated due to severe oxygen limitation 340 min after inoculation. In total, both phases contained 0.82 g RL. However, the supplied glucose was not fully converted, resulting in a yield of $0.02 \text{ g}_{\text{RL}} \text{ g}_{\text{Glc}}^{-1}$ if the remaining glucose is regarded as waste. Consequently, the RL production neither reached the anticipated production rate ($0.02 \text{ vs. } 0.13 \text{ g}_{\text{RL}} \text{ L}^{-1} \text{ h}^{-1}$) nor yield ($0.02 \text{ vs. } 0.12 \text{ g}_{\text{RL}} \text{ g}_{\text{Glc}}^{-1}$) of the benchmark two-liquid phase cultivation in the STR [14]. The main bottleneck and highest potential for improvement were determined to be the maximal *OTR*.

3.2 Evenly distributed small bubbles increase the oxygen transfer

To improve the *OTR* and thereby remedy the oxygen limitation as observed in the initial cultivation, the efficiency of the aeration was evaluated. The straightforward solution, the use of oxygen-enriched air, has not been assessed because of increasing fire hazards and operating costs. Instead, different sparger designs were tested to decrease the d_{32} of the bubbles, which is inversely proportional to the *OTR*.

The ring sparger with relatively large holes of 1 mm (Fig. 2a) dispersed bubbles with constant but high d_{32} of around 7.5 mm for all tested aeration rates from 0.5 to 3 vvm (cf. Fig. 5). To increase the volumetric surface area of the bubbles a metal sintered frit (Fig. 2b) was installed as a first measure. The frit sparger, consisting of finely porous metal, dispersed smaller and more homogeneous bubbles than the ring sparger. However, bubble sizes of the frit sparger increased almost linearly with increasing aeration rate from a comparatively low d_{32} of 2.1 mm at 0.5 vvm to 6.0 mm at 3 vvm. During the experiment, coalescence could be observed at higher aeration rates resulting in outliers as marked in the box plot for

Fig. 5 Bubble size distributions directly above the spargers (Ring, Frit, PAM, cf. Fig. 2) in predefined volume for aeration rates from 0.5 to 3 vvm. Depending on the aeration rate and sparger, 10 to 108 bubbles were evaluated in each experiment



an aeration rate of 3 vvm at 8.7 mm. This was due to a local higher holdup with smaller distances between the bubbles by dispersing the same gas volume through a smaller cross-sectional area. These coalesced bubbles have a significantly increasing impact on the d_{32} due to the cubic and quadratic relation between a sphere's diameter and volume, *i.e.*, bigger bubbles have an unproportionally higher impact on the volumetric surface area than smaller bubbles (Eq. (4)).

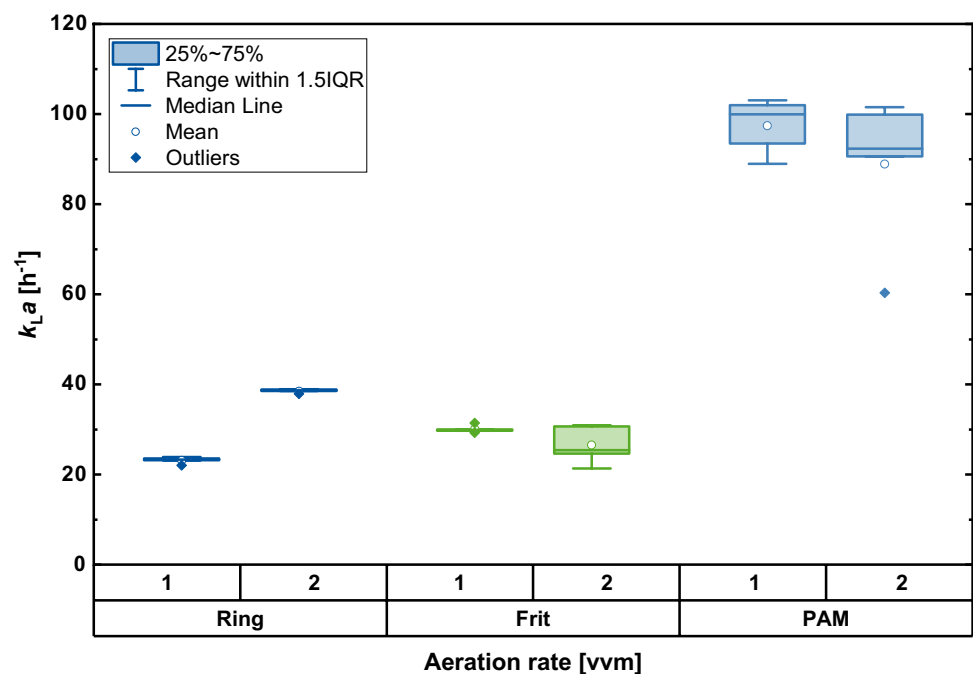
Increasing $k_L a$ -values are expected with decreasing bubble sizes and increasing aeration rates. The effect of bubble sizes can be shown by comparing the $k_L a$ -values, *e.g.*, between ring and frit sparger at the lowest assessed aeration rate of 1 vvm (Fig. 6). The $k_L a$ -value of the frit sparger (30.1 h^{-1}) was measured to be 28% higher compared to the $k_L a$ -value of the ring sparger (23.3 h^{-1}). However, regarding the aeration rate, the increase from 0.5 vvm to 3 vvm also increased the d_{32} of the bubbles supplied by the frit sparger approximately linearly. Although a higher $k_L a$ -value is expected due to higher aeration rates, this increase of the d_{32} acts contrarily, resulting in a lower $k_L a$ -value. In fact, the $k_L a$ -value of the reactor setup operated at 2 vvm with the frit sparger (26.6 h^{-1}) is even lower than the $k_L a$ -value when the ring sparger is installed (38.6 h^{-1}), although the d_{32} of the bubbles from the frit sparger is smaller than the d_{32} of the bubbles from the ring sparger.

Neither dispersing over the larger cross-sectional area spanned by the ring sparger nor dispersing small bubbles through the porous structure of the frit sparger sufficiently increased the *OTR*. Consequently, to combine these features, a 3D-printed PAM sparger was designed and constructed (*cf.* Fig. 2c). Combining a large cross-sectional area with a porous structure for smaller bubbles in the PAM sparger resulted in a homogenous holdup distribution across the cross-sectional area of the MPLR and therefore in less coalescence of the finely dispersed bubbles. The bubbles dispersed by the PAM sparger were distributed evenly and at a constant low d_{32} of about 2.5 mm, unaffected by the aeration rate (Fig. 5). Additionally, the PAM sparger produced a narrow bubble size distribution for all tested aeration rates. These improvements introduced by the PAM sparger resulted in $k_L a$ -values two- to threefold higher (95 h^{-1} , Fig. 6) compared to aeration with the ring sparger, with almost no influence by the rate of aeration.

3.3 The redesigned sparger facilitates sufficient oxygen supply for a successful batch cultivation

To alleviate the limited oxygen supply observed during the first cultivation in the MPLR, the original ring sparger was exchanged with the 3D-printed PAM sparger. The improved cultivation setup successfully allowed the maintenance of the *DOT* in the riser at above 50% via manual regulation during the whole cultivation period of about 13 h. Accordingly, the specific aeration rate was increased stepwise from 0.6 to 2.3 vvm whenever the *DOT* reached the lower boundary of 50% in the riser (Fig. 7a).

Fig. 6 $k_L a$ -values for aeration rates of 1 and 2 vvm and assessed spargers (Ring, Frit, PAM, *cf.* Fig. 2) in the MPLR



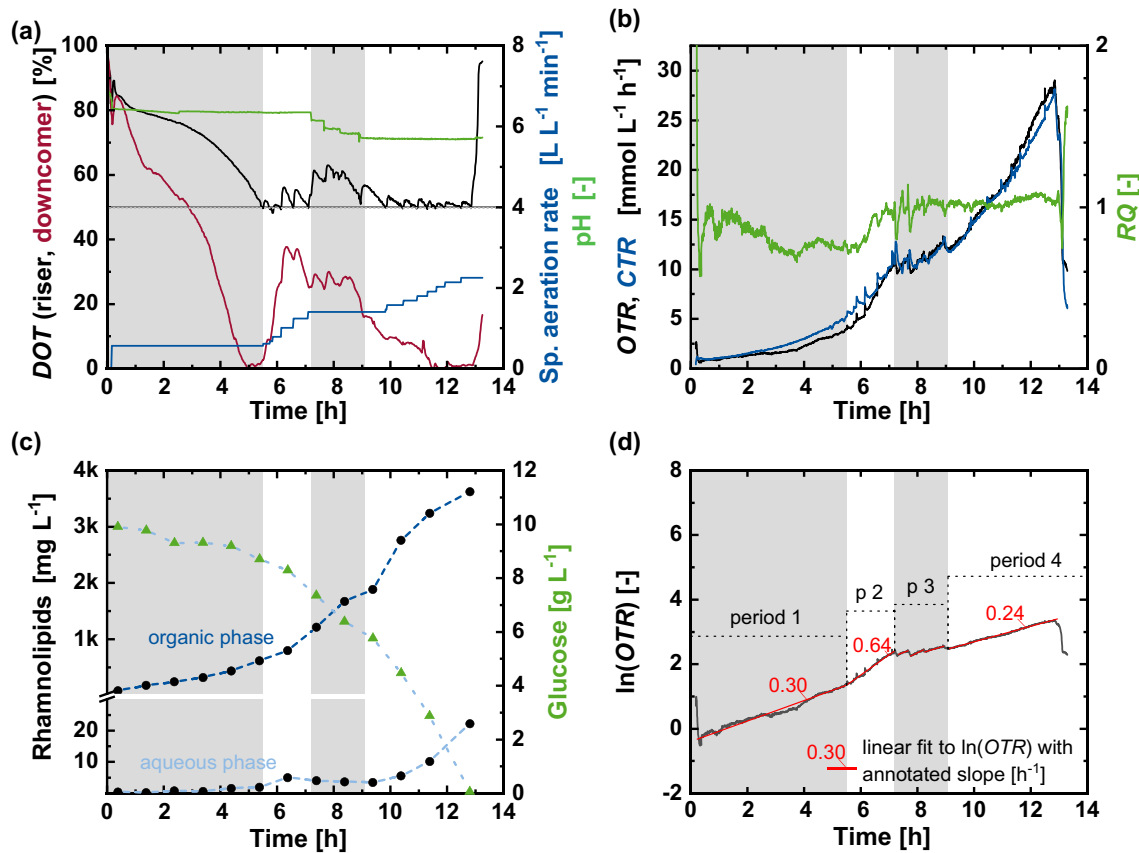


Fig. 7 Measured data of cultivation with PAM sparger with **a** DOTs, specific aeration rate, pH, **b** OTR, CTR, RQ **c** concentration of glucose (green triangles) and RLs (black dots) in aqueous (light blue dashes) and organic phases (dark blue dashes), and **d** the logarithmic OTR with linear fits and marked slopes over time. The shaded background mark periods annotated in **d** depend on the slope of the linear fit to $\ln(OTR)$

During this cultivation the organism exhibited four periods of different oxygen consumption rates, which are observable in the slope of the logarithmic OTR depicted in Fig. 7d. Neglecting the oxygen storage capability in the medium, the OTR equals the OUR. Therefore, the slope of the logarithmic OTR correlates with the growth rate, which, in turn, influences the production rate of the organism, as presented in the data.

Referring to the marked periods in the course of the logarithmic OTR, period 1 is dominated by a relatively low slope of 0.30 h^{-1} compared to 0.45 h^{-1} for the benchmark STR at the same pH value [14]. However, comparing the slope of period 1 to period 2 reveals that increasing the aeration rate led to an elevated slope of 0.64 h^{-1} compared to the benchmark. Therefore, it is hypothesized that the additional mixing effect due to an increased velocity of the loop flow at higher aeration rates positively affected the organism's metabolic state. The better mixing is underlined by the increase of the DOT in the downcomer in period 2 (Fig. 7, p 2) close to leveling up with the controlled DOT in the riser.

Starting with period 3 (p 3) excessive foaming required a stepwise reduction of the pH from 6.3 to 5.7. Thus, impairment due to foaming could be prevented. However, referring to Fig. 7b and c, RL production, glucose consumption, and data from the exhaust gas analytics substantially deviated from an exponential course during this period. Also, coinciding with each addition of sulfuric acid, the DOTs in the riser and downcomer increased although the aeration remained unaltered (Fig. 7a). This indicates increased stress for the cells by a reduction of the pH value and potential pH gradients. The stress and subsequent recovery of the cells caused by the addition of acid are also reflected in the logarithmic OTR. When the pH remained unaltered at a value of 5.7 after 8.5 h (p 3), the slope of the logarithmic OTR stabilized at 0.24 h^{-1} until glucose depletion. The lower value compared to previous phases is due to the deviation from an optimal pH range for *P. putida* KT2440 [14].

During the whole cultivation, the RQ ranged from 0.7 to 1.1 indicating glucose consumption. The concentrations of gluconate and 2-ketogluconate stayed below 0.5 g L^{-1} (Supplementary Information, Figure S2) and were depleted after 12.8 h simultaneously with glucose. The RL concentration stayed below 25 mg L^{-1} in the aqueous phase during the whole cultivation

by successfully accumulating the RL in the circulating organic phase to a titer of 3.6 g L^{-1} . A product yield of $0.11 \text{ g}_{\text{RL}} \text{ g}_{\text{Glc}}^{-1}$ and a productivity of $0.08 \text{ g}_{\text{RL}} \text{ L}^{-1} \text{ h}^{-1}$ were achieved.

4 Discussion and outlook

Previously, a two-liquid phase cultivation for the production of RL with recombinant *P. putida* in a bench-scale STR was developed [14]. In fact, besides the reactor, the cultivations including strain, extraction solvent, and media composition in the presented study were identical to the mentioned STR cultivation. While yields were similar in both systems (MPLR: $0.11 \text{ g}_{\text{RL}} \text{ g}_{\text{Glc}}^{-1}$, STR: $0.12 \text{ g}_{\text{RL}} \text{ g}_{\text{Glc}}^{-1}$), the productivity in the MPLR was lower (MPLR: $0.08 \text{ g}_{\text{RL}} \text{ L}^{-1} \text{ h}^{-1}$, STR: $0.13 \text{ g}_{\text{RL}} \text{ L}^{-1} \text{ h}^{-1}$). The reduced productivity is most likely due to two reasons revealed in this study, which urge two major aspects for improvement: (1) A more gradual addition of acid and base to a region of high turbulence to avoid gradients when adjusting the pH value, and (2) increasing the power input for better mixing and an enhanced loop flow velocity by a higher aeration rate to elevate the overall metabolic activity. The production of RL in STRs in dynamic batch or fed-batch modes requires an ongoing decrease of the pH value, thereby increasingly diverging from an optimal range, which has been shown to restrict growth and production. Phase separation as a prerequisite for a continuous mode is impracticable for two-liquid phase cultivations in STRs producing RL due to stable emulsions caused by high shear rates resulting from agitation [14]. In the MPLR, however, continuous separation of the extraction solvent is possible enabling a fully continuous mode of operation. As the RL can be removed from the system, the continuous cultivation can reach a steady state, and consequently, the pH does not need to be lowered to an unfavorable level.

Other cultivation strategies for RL production involve external loops for directed foaming-out and partial foam fractionation [37, 38]. A rather long loop trajectory potentially results in performance-diminishing high anaerobic residence times or even a loss of the whole-cell biocatalyst. However, in the MPLR, anaerobic residence times are minimized due to a short trajectory of the cells in the non-actively aerated downcomer. Furthermore, the process-intensifying MPLR spares space and equipment compared to, e.g., a directed outflow of the foam requiring highly voluminous tanks of multiple sizes of the actual reactor [4]. The operation of the MPLR only requires a small additional solvent storage tank, smaller in size compared to the reactor itself.

While demonstrated for the production of RL, the MPLR bears the potential for applications in bioprocesses with other whole-cell biocatalysts synthesizing various products. Due to the *in situ* liquid-liquid extraction, the MPLR can be particularly advantageous for product-inhibited bioprocesses [39], especially when operated in continuous mode. Due to the lower and more homogeneously dissipated shear stress compared to STRs, organisms that are more shear-sensitive than bacteria, such as mammalian, insect, or plant cells [23], can be cultivated. Performing a variety of different bioprocesses in the reactor establishes the reactor as a platform technology in the bioeconomy.

However, further research and development are required to reduce the technological risks. This study forms an intermediate step towards a fully continuous fermentation. The material system previously established in STRs was successfully transferred to the MPLR. Due to the dynamic nature of the batch mode performed here, various operating points were tested over a period of time. A fully continuous operation can be achieved by an additional feed and purge for the aqueous phase, as well as a continuous removal and addition of solvent to the solvent circuit. Once established it may reveal further insights into the genetic stability of the microorganism and instabilities of the overall system and may indicate the limit of practically possible space-time yield.

Furthermore, relations of fluid dynamics to aeration and extraction as well as ideal geometrical parameters such as filling volume and riser-to-downcomer ratio need to be determined. Additionally, turbulences and laminar or stagnant zones need to be localized, potentially leading to a refinement of the geometrical design. The refined setup can subsequently be applied in a continuous cultivation, ideally including an adjacent online solvent recovery unit. Further, insights into the scalability of the MPLR need to be gained, and an economic evaluation in comparison to conventional cultivation systems has to be conducted. Ongoing improvement, customization, and evaluation of the MPLR will increase its technology readiness level and establish it as a platform technology for bioprocesses.

5 Conclusion

The advancement of the envisaged bioeconomy is rapidly progressing, and it has underlined its enormous potential to contribute to circular, zero-waste resource utilization. With increasing complexity and requirements of processes and whole-cell biocatalysts, specialized process solutions, including tailored bioreactors, are demanded. In this regard, the

functionality of the MPLR for sustaining a microbial bioprocess with integrated *in situ* extraction with continuous solvent removal was demonstrated in this work. Excessive foaming during the production of RL was prevented while performing equally well as reference cultivations in STRs with the advantage of allowing full continuous mode. By further refining and tailoring the MPLR for challenging bioprocesses it bears the potential to advance into a platform technology and thereby support the transformation towards a circular bioeconomy in the future.

Acknowledgements The authors thank Steffen Dietz and Tammo Schüler for experimental support and Katharina Saur and Tobias Karmainski for proofreading the manuscript.

Author contributions All experiments: MVC, PD. Seed cultures, media preparation, and analytics: PD. Sparger construction: AS, PB. Interpreted results: MVC, PD, PB, TT, LMB, AJ, MW. Drafted the manuscript: MVC, PD. Revised and edited the manuscript: TT, LMB, AJ, MW. All authors commented on the manuscript before publication. All authors read and approved the final manuscript.

Funding Open Access funding enabled and organized by Projekt DEAL. The project on which this report is based was funded by the German Federal Ministry of Education and Research (BMBF) under the funding codes 031B0350A and 031B0350B. The PAM sparger was financed by the Innovation Sprint of the RWTH Aachen Innovation by the 'Excellence Start-up Center.NRW' initiative, funded by the state of North Rhine-Westphalia. The sponsor is the Ministry of Economy, Innovation, Digitization and Energy. The laboratories of AJ, LMB and MW were partially funded by the German Research Foundation (DFG) under Germany's Excellence Strategy within the Cluster of Excellence FSC 2186 'The Fuel Science Center' (ID: 390919832). The responsibility for the content of this publication lies with the authors.

Data availability The datasets generated during and/or analyzed during the current study are available from the corresponding author on reasonable request.

Declarations

Competing interests AJ declares that he is inventor of the related patent: A. Bednarz, A. Jupke, M. Schmidt and B. Weber, "Mehrphasenschlaufenreaktor und Verfahren zum Betrieb", RWTH Aachen University, 2017 (PCT/EP2017/054967). LMB and TT declare that they are inventors of three related patents. 1) L. M. Blank, F. Rosenau, S. Wilhelm, A. Wittgens, T. Tiso, "Means and methods for rhamnolipid production", HHU Düsseldorf University, TU Dortmund University, 2013 (WO 2013/041670 A1), 2) L. M. Blank, B. Küpper, E. M. del Amor Villa, R. Wichmann, C. Nowacki, "Foam adsorption", TU Dortmund University, 2013 (WO 2013/087674 A1), and 3) L. M. Blank, T. Tiso, A. Germer, "Extracellular production of designer hydroxyalkanoyloxy alkanolic acids with recombinant bacteria", RWTH Aachen University, 2015 (WO2017006252A1). PB, AS and MW declare that they are inventors at the patent application "Verfahren zur Additiven Fertigung poröser gasdurchlässiger Formkörper mit steuerbarer Porosität" (filed with the German Patent and Trademark Office on 30/06/2021; official file number: 10 2021 116 862.7). Apart from that, the authors declare that the research was conducted in the absence of any commercial or financial relationships that could be construed as a potential conflict of interest.

Open Access This article is licensed under a Creative Commons Attribution 4.0 International License, which permits use, sharing, adaptation, distribution and reproduction in any medium or format, as long as you give appropriate credit to the original author(s) and the source, provide a link to the Creative Commons licence, and indicate if changes were made. The images or other third party material in this article are included in the article's Creative Commons licence, unless indicated otherwise in a credit line to the material. If material is not included in the article's Creative Commons licence and your intended use is not permitted by statutory regulation or exceeds the permitted use, you will need to obtain permission directly from the copyright holder. To view a copy of this licence, visit <http://creativecommons.org/licenses/by/4.0/>.

References

1. Vardar-Sukan F. Foaming: consequences, prevention and destruction. *Biotechnol Adv.* 1998. [https://doi.org/10.1016/S0734-9750\(98\)00010-X](https://doi.org/10.1016/S0734-9750(98)00010-X).
2. Varley J, Brown AK, Boyd J, Dodd PW, Gallagher S. Dynamic multi-point measurement of foam behaviour for a continuous fermentation over a range of key process variables. *Biochem Eng J.* 2004. <https://doi.org/10.1016/j.bej.2004.02.012>.
3. Tiso T. Foaming in biotechnological processes – Challenges and opportunities (in preparation). *Discover Chem. Eng.* 2022.
4. Bator I, Karmainski T, Tiso T, Blank LM. Killing two birds with one stone – Strain engineering facilitates the development of a unique rhamnolipid production process. *Front Bioeng Biotechnol.* 2020. <https://doi.org/10.3389/fbioe.2020.00899>.
5. Delvigne F, Lecomte J. Foam formation and control in bioreactors. In: Flickinger MC, editor. *Encyclopedia of industrial biotechnology*. Hoboken: Wiley; 2009.
6. Bongartz P, Bator I, Baitalow K, Keller R, Tiso T, Blank LM, Wessling M. A scalable bubble-free membrane aerator for biosurfactant production. *Biotechnol Bioeng.* 2021. <https://doi.org/10.1002/bit.27822>.
7. Beuker J, Barth T, Steier A, Wittgens A, Rosenau F, Henkel M, Hausmann R. High titer heterologous rhamnolipid production. *AMB Express.* 2016. <https://doi.org/10.1186/s13568-016-0298-5>.
8. Anic I, Apollonia I, Franco P, Wichmann R. Production of rhamnolipids by integrated foam adsorption in a bioreactor system. *AMB Express.* 2018. <https://doi.org/10.1186/s13568-018-0651-y>.

9. Blesken CC, Strümpfler T, Tiso T, Blank LM. Uncoupling foam fractionation and foam adsorption for enhanced biosurfactant synthesis and recovery. *Microorganisms*. 2020. <https://doi.org/10.3390/microorganisms8122029>.
10. Freeman A, Woodley JM, Lilly MD. *In situ* product removal as a tool for bioprocessing. *Biotechnology (N Y)*. 1993. <https://doi.org/10.1038/nbt0993-1007>.
11. López-Garzón CS, Straathof AJJ. Recovery of carboxylic acids produced by fermentation. *Biotechnol Adv*. 2014. <https://doi.org/10.1016/j.biotechadv.2014.04.002>.
12. Badhwar P, Kumar P, Dubey KK. Extractive fermentation for process integration and amplified pullulan production by *A. pullulans* in aqueous two phase systems. *Sci Rep*. 2019. <https://doi.org/10.1038/s41598-018-37314-y>.
13. Verhoef S, Wierckx N, Westerhof RGM, de Winde JH, Ruijsseenaars HJ. Bioproduction of *p*-hydroxystyrene from glucose by the solvent-tolerant bacterium *Pseudomonas putida* S12 in a two-phase water-decanol fermentation. *Appl Environ Microbiol*. 2009. <https://doi.org/10.1128/AEM.02186-08>.
14. Demling P, von Campenhausen M, Grütering C, Tiso T, Jupke A, Blank LM. Selection of a recyclable *in situ* liquid-liquid extraction solvent for foam-free synthesis of rhamnolipids in a two-phase fermentation. *Green Chem*. 2020. <https://doi.org/10.1039/D0GC02885A>.
15. Pappas T, Oudshoorn A. Enabling cost effective butanol production with DAB.bio's unique bioreactor technology. Latest updates and news. DAB. 2022. <https://dab.bio/wp-content/uploads/2022/03/DAB.bio-butanol-tech-report.pdf>. Accessed 30 Aug 2022.
16. Teke GM, Pott RWM. Design and evaluation of a continuous semipartition bioreactor for *in situ* liquid-liquid extractive fermentation. *Biotechnol Bioeng*. 2021. <https://doi.org/10.1002/bit.27550>.
17. Hanson C. Recent advances in liquid-liquid extraction. Oxford: Pergamon; 1975.
18. Chen HT, Middleman S. Drop size distribution in agitated liquid-liquid systems. *AIChE J*. 1967. <https://doi.org/10.1002/aic.690130529>.
19. Dorobantu LS, Yeung AKC, Foght JM, Gray MR. Stabilization of oil-water emulsions by hydrophobic bacteria. *Appl Environ Microbiol*. 2004. <https://doi.org/10.1128/AEM.70.10.6333-6336.2004>.
20. Chen D, Pu B. Studies on the Binary Coalescence Model. *J Colloid Interface Sci*. 2001. <https://doi.org/10.1006/jcis.2001.7817>.
21. Bednarz A, Jupke A, Schmidt M, Weber B, inventors; Rheinisch-Westfälische Technische University (RWTH) Aachen. Multi-phase loop reactor and method of operation. 2017 Mar 2.
22. Guieysse B, Quijano G, Muñoz R. Airlift bioreactors. In: comprehensive biotechnology. Amsterdam: Elsevier; 2011. p. 199–212.
23. Reay D, Ramshaw C, Harvey A. Chapter 2 - Process intensification – an overview. In: Reay D, Ramshaw C, Harvey A, editors. Process intensification. Oxford: Butterworth-Heinemann; 2008. p. 21–45.
24. Demling P, Ankenbauer A, Klein B, Noack S, Tiso T, Takors R, Blank LM. *Pseudomonas putida* KT2440 endures temporary oxygen limitations. *Biotechnol Bioeng*. 2021. <https://doi.org/10.1002/bit.27938>.
25. Tiso T, Zauter R, Tulke H, Leuchtle B, Li W-J, Behrens B, Wittgens A, Rosenau F, Hayen H, Blank LM. Designer rhamnolipids by reduction of congener diversity: production and characterization. *Microb Cell Fact*. 2017. <https://doi.org/10.1186/s12934-017-0838-y>.
26. Wittgens A, Tiso T, Arndt TT, Wenk P, Hemmerich J, Müller C, Wichmann R, Küpper B, Zwick M, Wilhelm S, Hausmann R, Sylđatk C, Rosenau F, Blank LM. Growth independent rhamnolipid production from glucose using the non-pathogenic *Pseudomonas putida* KT2440. *Microb Cell Fact*. 2011. <https://doi.org/10.1186/1475-2859-10-80>.
27. Bongartz P, Scheele A, Matthias W, inventors; Rheinisch-Westfälische Technische University (RWTH) Aachen. Verfahren zur Additiven Fertigung poröser gasdurchlässiger Formkörper mit steuerbarer Porosität.
28. Bagdasarian M, Lurz R, Rückert B, Franklin F, Bagdasarian MM, Frey J, Timmis KN. Specific-purpose plasmid cloning vectors II. Broad host range, high copy number, RSF 1010-derived vectors, and a host-vector system for gene cloning in *Pseudomonas*. *Gene*. 1981. [https://doi.org/10.1016/0378-1119\(81\)90080-9](https://doi.org/10.1016/0378-1119(81)90080-9).
29. Kampers LFC, Volkers RJM, dos Santos M, Vitor AP. *Pseudomonas putida* KT2440 is HV1 certified, not GRAS. *Microb Biotechnol*. 2019. <https://doi.org/10.1111/1751-7915.13443>.
30. Nakazawa T. Travels of a *Pseudomonas*, from Japan around the world. *Environ Microbiol*. 2002. <https://doi.org/10.1046/j.1462-2920.2002.00310.x>.
31. Hartmans S, Smits JP, van der Werf MJ, Volkering F, de Bont JAM. Metabolism of styrene oxide and 2-phenylethanol in the styrene-degrading *Xanthobacter* Strain 124X. *Appl Environ Microbiol*. 1989. <https://doi.org/10.1128/aem.55.11.2850-2855.1989>.
32. Bator I, Wittgens A, Rosenau F, Tiso T, Blank LM. Comparison of three xylose pathways in *Pseudomonas putida* KT2440 for the synthesis of valuable products. *Front Bioeng Biotechnol*. 2020. <https://doi.org/10.3389/fbioe.2019.00480>.
33. Whitman WG. The two film theory of gas absorption. *Int J Heat Mass Transfer*. 1962. [https://doi.org/10.1016/0017-9310\(62\)90032-7](https://doi.org/10.1016/0017-9310(62)90032-7).
34. Meusel W, Löffelholz C, Husemann U, Dreher T, Greller G, Kauling J, Eibl D, Kleebank S, Bauer I, Glöckler R, Huber P, Kuhlmann W, John GT, Werner S, Kaiser SC, Pörtner R, Kraume M. Recommendations for process engineering characterisation of single-use bioreactors and mixing systems by using experimental methods. Studien und Positionspapiere. DECHEMA Gesellschaft für Chemische Technik und Biotechnologie e.V. 2016. https://dechema.de/dechema_media/Downloads/Positionspapiere/SingleUse_ProcessEngineeringCharacterisation_2016.pdf. Accessed 10 Mar 2021.
35. Mießner U, Kück UD, Dujardin V, Heithoff S, Rübiger N. Correlation for *k*_La prediction of Airlift loop reactors including the gas phase residence time effect. *Chem Eng Technol*. 2015. <https://doi.org/10.1002/ceat.201500154>.
36. Sauter J. Die Größenbestimmung der im Gemischnebel von Verbrennungskraftmaschinen vorhandenen Brennstoffteilchen. München: VDI-Verlag; 1926.
37. Blesken CC, Bator I, Eberlein C, Heipieper HJ, Tiso T, Blank LM. Genetic cell-surface modification for optimized foam fractionation. *Front Bioeng Biotechnol*. 2020. <https://doi.org/10.3389/fbioe.2020.572892>.
38. Merz J. A contribution to design foam fractionation processes. Dortmund: Technische Universität Dortmund; 2012.
39. van Hecke W, Kaur G, de Wever H. Advances in *in-situ* product recovery (ISPR) in whole cell biotechnology during the last decade. *Biotechnol Adv*. 2014. <https://doi.org/10.1016/j.biotechadv.2014.07.003>.